Biochimica et Biophysica Acta 1863 (2016) 2637–2649

Contents lists available at ScienceDirect

Biochimica et Biophysica Acta

journal homepage: www.elsevier.com/locate/bbamcr

In vitro aging promotes endoplasmic reticulum (ER)-mitochondria Ca^{2+} cross talk and loss of store-operated Ca^{2+} entry (SOCE) in rat hippocampal neurons

María Calvo-Rodríguez [a,1], Mónica García-Durillo [a], Carlos Villalobos [a,*], Lucía Núñez [a,b]

[a] Instituto de Biología y Genética Molecular (IBGM), Consejo Superior de Investigaciones Científicas (CSIC), Valladolid, Spain
[b] Departamento de Bioquímica y Biología Molecular y Fisiología, Universidad de Valladolid, Valladolid, Spain

ARTICLE INFO

Article history:
Received 23 February 2016
Received in revised form 27 July 2016
Accepted 4 August 2016
Available online 5 August 2016

Keywords:
Aging
Hippocampal neurons
Store-operated calcium entry
ER-mitochondria cross talking
Stim1
Orai1

ABSTRACT

Aging is associated to cognitive decline and susceptibility to neuron death, two processes related recently to subcellular Ca^{2+} homeostasis. Memory storage relies on mushroom spines stability that depends on store-operated Ca^{2+} entry (SOCE). In addition, Ca^{2+} transfer from endoplasmic reticulum (ER) to mitochondria sustains energy production but mitochondrial Ca^{2+} overload promotes apoptosis. We have addressed whether SOCE and ER-mitochondria Ca^{2+} transfer are influenced by culture time in long-term cultures of rat hippocampal neurons, a model of neuronal aging. We found that short-term cultured neurons show large SOCE, low Ca^{2+} store content and no functional coupling between ER and mitochondria. In contrast, in long-term cultures reflecting aging neurons, SOCE is essentially lost, Stim1 and Orai1 are downregulated, Ca^{2+} stores become overloaded, Ca^{2+} release is enhanced, expression of the mitochondrial Ca^{2+} uniporter (MCU) increases and most Ca^{2+} released from the ER is transferred to mitochondria. These results suggest that neuronal aging is associated to increased ER-mitochondrial cross talking and loss of SOCE. This subcellular Ca^{2+} remodeling might contribute to cognitive decline and susceptibility to neuron cell death in the elderly.

1. Introduction

Aging is associated to cognitive decline and increased risk of neuron cell death related to excitotoxicity and/or neurodegenerative diseases. These processes have been linked to the remodeling of intracellular Ca^{2+} homeostasis including changes in voltage-gated Ca^{2+} channels and glutamate receptors sensitive to *N*-Methyl-D-Aspartate (NMDA). Interestingly, some of these changes are mimicked *in vitro* after long-term culture of rat hippocampal neurons [1,2]. In fact, after several weeks in culture, rat hippocampal neurons display important hallmarks of neuronal aging *in vivo* including accumulation of reactive oxygen species (ROS), lipofuscin granules, heterochromatic foci, activation of the Jun N-terminal protein kinase (pJNK) and p53/p21 pathways, gradual loss of cholesterol, and, as stated above, changes in Ca^{2+} channel density and NMDA receptor expression [1–5]. Accordingly, long-term cultures of hippocampal neurons may provide a suitable model for investigating Ca^{2+} remodeling in aging hippocampal neurons.

In the last few years, it has been reported that memory storage in the hippocampus depends on store-operated Ca^{2+} entry (SOCE) which is required for mushroom spines stability [6]. SOCE is triggered by the release of Ca^{2+} from intracellular stores induced by phospholipase C activation after receptor stimulation [7]. At the molecular level, SOCE is induced by interaction of stromal interaction molecule 1 (Stim1) [8], a Ca^{2+} sensor at the endoplasmic reticulum (ER), and Orai1, a pore forming protein of store-operated channels (SOCs) at the plasma membrane [9,10]. SOCE has been studied in detail in non-excitable cells. However, it is also present in excitable cells including neurons [7,11]. It has been proposed that the Ca^{2+} sensor at ER that triggers SOCE in hippocampal neurons is Stim2 rather than Stim1 [12]. However, this view is controversial and recent results indicate that both Stim proteins are involved in Ca^{2+} homeostasis in neurons. STIM1 mainly activates SOCE, whereas Stim2 regulates resting Ca^{2+} levels in the ER and Ca^{2+} leakage with the additional involvement of Stim1 [13]. Interestingly, recent data suggest that Stim2 is downregulated in aging animals, animal models of AD and AD patients [6] suggesting an important role of Stim2 and SOCE in aging and AD.

Subcellular Ca^{2+} homeostasis is critical for neuron cell damage induced by different insults including excitotoxicity and neurodegeneration. For example, activation of NMDA receptors promotes mitochondrial Ca^{2+} overload and cell death in long-term cultured hippocampal neurons [4,5]. Likewise, oligomers of the amyloid β peptide (Aβ), the most likely neurotoxin in AD, promote Ca^{2+} entry, mitochondrial Ca^{2+} overload and neuron cell death in

* Corresponding author.
E-mail address: carlosv@ibgm.uva.es (C. Villalobos).
[1] Present address: Alzheimer Research Unit, Department of Neurology, Massachusetts General Hospital and Harvard Medical School, 114, 16th St. Charlestown, MA 02129, USA.

http://dx.doi.org/10.1016/j.bbamcr.2016.08.001
0167-4889/

cerebellar granule cells [14]. Both Aβ and NMDA promote Ca^{2+} influx but they also mobilize Ca^{2+} from stores. Specifically, Aβ mobilizes ER Ca^{2+} *via* IP_3 dependent and independent mechanisms [15]. Aβ and NMDA receptor activation cause mitochondrial dysfunction involving ER Ca^{2+} release [16]. These findings suggest a relevant role for Ca^{2+} transfer from ER to mitochondria in neuron cell death. The role of Ca^{2+} transfer from ER to mitochondria in aging has not been addressed. In fact, mitochondria Ca^{2+} handling has remained elusive due to the constrains of monitoring accurately mitochondrial Ca^{2+} concentration ($[Ca^{2+}]_{mit}$) in individual neurons. However, bioluminescence imaging of targeted probes like aequorin has revealed the presence of subpopulations of mitochondria able to sense high Ca^{2+} domains (Ca^{2+} microdomains) near Ca^{2+} channels at the plasma membrane [17,18] and the ER [19,20]. More recent data indicates that Ca^{2+} transfer from ER to mitochondria depends on the formation of close contacts sites between ER and mitochondria [21] and specialized structures named mitochondria-associated membranes (MAMs) [22,23]. Ca^{2+} transfer from the ER to mitochondria is involved in cell survival as well. Absence of this transfer results in enhanced phosphorylation of pyruvate dehydrogenase and AMP kinase (AMPK) activation, promoting prosurvival macroautophagy. Thus, constitutive $InsP_3R$ dependent Ca^{2+} release to mitochondria is an essential cellular process required for efficient mitochondrial respiration and maintenance of bioenergetics [24]. Whether this transfer is affected by aging has not been addressed. Inasmuch as mitochondrial potential ($\Delta\Psi$), the main driving force for mitochondrial Ca^{2+} uptake, decreases with age [4,25], it is possible that aging may influence Ca^{2+} transfer from ER to mitochondria. Here we have used long-term cultures of rat hippocampal neurons to address whether SOCE and ER–mitochondria Ca^{2+} cross talk are influenced by *in vitro* aging.

2. Methods

2.1. Animals and reagents

Wistar rat pups were obtained from the Valladolid University animal facility. All animals were handled according to ethical standards approved by the animal housing facility of the Valladolid University Medical School (Valladolid, Spain) in agreement with the European Convention 123/Council of Europe and Directive 86/609/EEC. Fura2/AM, TMRM, coelenterazine and lipofectamine® 2000 are from Invitrogen (Barcelona, Spain). Fetal bovine serum (FBS) is from Lonza (Barcelona, Spain). Horse serum, neurobasal medium, HBSS medium, B27, L-glutamine and gentamicin are from Gibco (Barcelona, Spain). Papain solution is from Worthington (Lakewood, NJ). The poly-D-lysine and Annexin V are from BD (Madrid, Spain). DNase I and antibody against mitochondrial calcium uniporter (MCU) are from Sigma (Madrid, Spain). Antibodies against Stim1 and Orai1 are from Alomone (Jerusalem, Israel). Antibody against βIII tubulin is from Covance (Princeton, NJ, USA). Other reagents and chemicals were obtained either from Sigma or Merck. Plasmids for mitochondria-targeted aequorin fused to GFP are a kind gift from Prof. P. Brulet (CNRS, France).

2.2. Primary hippocampal neuron culture

Hippocampal neurons were prepared from Wistar rat pups under sterile conditions as reported by Brewer et al. [26] with further modifications by Perez-Otaño et al. [27]. Briefly, newborn rat pups were decapitated and, after brain removal, meninges were discarded and hippocampi were separated from cortex. Hippocampal tissue was cut in small pieces, transferred to papain solution (20 u/ml) and incubated at 37 °C for 30 min. After 15 min, DNase I (50 μg/ml) was added. Tissue pieces were washed with Neurobasal Medium and cell suspension was obtained using a fire-polished pipette in the same medium supplemented with 10% FBS. Cells were centrifuged at 160*g* for 5 min and pellet was suspended in Neurobasal medium. Hippocampal cells were plated onto poly-D-lysine-coated, 12 mm diameter glass coverslips at 30×10^3 cells/dish (plating density, 169 cells/mm^2), and grown in Neurobasal medium supplemented with L-glutamine (2 mM), gentamicin (1 μg/ml), 2% B27 and 10% FBS, and maintained in a humidified incubator at 37 °C with 5% CO_2 without further media exchange. Cells were cultured for 4–8 days *in vitro* (DIV) for resembling "young" neurons or 15–21 DIV for mimicking "aged" neurons before experiments. Other details have been reported in detail elsewhere [4,28].

2.3. Fluorescence imaging of cytosolic free Ca^{2+} concentration

Hippocampal cells were cultured for 4–8 DIV or 15–21 DIV and washed in standard external medium (SEM) containing (in mM) NaCl 145, KCl 5, $CaCl_2$ 1, $MgCl_2$ 1, glucose 10 and Hepes/NaOH 10 (pH 7.4). Cells were incubated in the SEM containing fura2/AM (4 μM) for 60 min at room temperature in the dark. Then coverslips were placed on the perfusion chamber of a Zeiss Axiovert 100 TV inverted microscope, perfused continuously with pre-warmed (37 °C) SEM and epi-illuminated alternately at 340 and 380 nm light using a filter wheel. Light emitted at 520 nm was filtered with the dichroic mirror and recorded every 5 s with a Hamamatsu ER camera (Hamamatsu Photonics France). Pixel by pixel ratios of consecutive frames were captured and $[Ca^{2+}]_{cyt}$ values from regions of interest (ROIs) corresponding to individual neurons were averaged and expressed as the ratio of fluorescence emission following excitation at 340 and 380 nm as reported in detail previously [4,14]. For calculations of cytosolic $[Ca^{2+}]$ the Grynkiewicz equation was used: $[Ca^{2+}] = Kd * (R - Rmin) / (Rmax - R) * F380max/F380min$ [29] where Kd is the dissociation constant of fura2 (224 nM), R is the observed fluorescence ratio at both wavelengths (F340/F380); Rmin is the minimum ratio value (in absence of Ca^{2+}); Rmax is the maximum ratio value (when Fura-2 is saturated by Ca^{2+}) and F380max/F380min is a scaling factor (fluorescence intensity at 380 nm excitation in the absence of Ca^{2+} and at Ca^{2+} saturation). We used the following values for our imaging setup: Rmax = 1.4; Rmin = 0.1, respectively. F380max/F380min = 2.7. For best comparison both ratios and calculated cytosolic $[Ca^{2+}]$ are shown.

For measurements of SOCE, fura2-loaded cells were treated with the sarcoplasmic and endoplasmic reticulum Ca^{2+} ATPase (SERCA) pump blocker thapsigargin (Tg, 1 μM) for 10 min in SEM devoid of extracellular Ca^{2+} before imaging. Then cells were subjected to fluorescence imaging and stimulated with 5 mM Ca^{2+} to monitor the SOCE-dependent rise in $[Ca^{2+}]_{cyt}$. SOCE recordings were made in the presence of tetrodotoxin (TTX) to prevent activation of voltage-gated Ca^{2+} channels by connected neurons. For estimation of Ca^{2+} store content, we measured the rise in $[Ca^{2+}]_{cyt}$ induced by low concentrations of the Ca^{2+} ionophore ionomycin (400 nM) added in the absence of extracellular Ca^{2+}. Ionomycin releases Ca^{2+} stored by making holes in endomembranes. Accordingly, the rise in $[Ca^{2+}]_{cyt}$ depends solely on the amount of stored Ca^{2+} and not on expression of G-protein coupled receptors and or IP_3 receptors. This procedure has been used extensively to estimate Ca^{2+} store content [11].

For quantification of rises in $[Ca^{2+}]_{cyt}$, the maximum rise in ratio was computed for responsive cells. In addition, we calculated the fraction of responsive cells. Finally, we calculated the product of the maximum rise in ratio by the fraction of responsive cells in order to have an estimation of the increase in $[Ca^{2+}]$ in response to a given agonist in the whole cell population. This procedure has been described in the same cells in detail previously [4].

2.4. Bioluminescence imaging of mitochondrial free Ca^{2+} concentration

Cultured neurons were transfected with the mitGA and mutated mitGA plasmids using lipofectamine® 2000. These plasmids contain wild type or mutated, low affinity aequorin targeted to mitochondria

and a GFP sequence to select transfected neurons for bioluminescence imaging. Transfection efficiency was 10–20%. After 24 h, cells were washed with SEM and incubated for 2 h with 4 μM coelenterazine at room temperature in the dark. Then, cells were washed again and placed into a perfusion chamber coupled to Zeiss Axiovert S100 TV inverted microscope. Cells were perfused at 5–10 ml/min with pre-warmed (37 °C) test solutions made in SEM. At the end of each experiment, cells were permeabilised with 0.1 mM digitonin solved in SEM containing 10 mM $CaCl_2$ in order to release all the residual photonic emissions, a value that is required for calibration. For permeabilisation, cells were treated with a digitonin 50 μM solved in intracellular standard medium (ISM) (130 mM KCl, 10 mM NaCl, 1 mM $MgCl_2$, 1 mM K_3PO_4, 0.2 mM EGTA, 1 mM ATP, 20 μM ADP, 2 mM succinate, and 20 mM HEPES, pH 6.8). Then, cells were incubated with ISM containing EGTA-buffered, low [Ca^{2+}] (200 nM) for 5 min before perfusing with ISM containing 10 μM [Ca^{2+}] for 1 min. This medium is intended to test mitochondrial Ca^{2+} uptake in the presence of a given rise in $[Ca^{2+}]_{cyt}$ large enough to promote mitochondrial Ca^{2+} uptake. Bioluminescence images were taken with a Hamamatsu VIM photon counting camera handled with an Argus-20 image processor. For analysis, regions of interest (ROIs) corresponding to individual neurons selected for their morphology and photonic emissions were integrated for 10 s periods and converted into values of mitochondria free Ca^{2+} concentration ($[Ca^{2+}]_{mit}$) as reported previously [17,18,28,30].

2.5. Mitochondrial potential

Hippocampal neurons were washed in SEM and loaded with the mitochondrial potential probe tetramethylrhodamine, methyl ester (TMRM, 10 nM) for 30 min at room temperature in the dark. Then coverslips containing cells were placed on a Zeiss Axiovert 100 TV inverted microscope and subjected to fluorescence imaging. Fluorescence images were captured with the rhodamine filter set with a Hamamatsu ER-Orca fluorescence camera as reported previously [4,14,31].

2.6. Immunofluorescence

Hippocampal cells in culture were fixed with *p*-formaldehyde 4% and incubated with antibodies against MCU (1:200), Stim1 (1:50), Orai1 (1:50) and βIII tubulin (1:300) at 4 °C overnight. Immunopositive cells were revealed using Alexafluor 488-tagged antibodies (1:300). Size of neurons in short-term and long-term cultured was different. Accordingly, fluorescence emission per area unit (optical density) was measured in selected ROIs corresponding to individual neurons using ImageJ software. Further details have been reported elsewhere [4].

2.7. Statistics

Changes in fluorescence ratio are expressed as A.U.C. (area under curve) and maximum increase in ratio (Δratio). Calculations were performed using Origin Lab 7.0. Data are presented as mean ± SEM. When only two means were compared, Student's *t*-test was used. For more than two groups, statistical significance of the data was assessed by one-way ANOVA and compared using Bonferroni's multiple comparison tests. Differences were considered significant at $p < 0.05$.

3. Results

3.1. In vitro aging downregulates store-operated Ca^{2+} entry in rat hippocampal neurons

Store-operated Ca^{2+} entry (SOCE), the Ca^{2+} entry pathway activated by the emptying of intracellular Ca^{2+} stores, was tested in 4–8 DIV and 15–21 DIV hippocampal neurons using fluorescence imaging. For this end, fura2-loaded hippocampal cells were treated with the SERCA pump blocker thapsigargin (Tg) in Ca^{2+} free medium to deplete intracellular Ca^{2+} stores. Then cells were subjected to fluorescence imaging and the effects of extracellular Ca^{2+} addition on $[Ca^{2+}]_{cyt}$ were monitored. Imaging experiments were carried out in the presence of tetrodotoxin (TTX) to prevent activation of the neural network formed *in vitro* and/or to Ca^{2+} entry secondary to activation of ligand and/or voltage-activated Ca^{2+} channels. Neurons were selected according to morphologic characteristics. Fig. 1 shows that addition of external Ca^{2+} to cells not treated with Tg induces an small rise in $[Ca^{2+}]_{cyt}$ that is similar in 4–8 DIV and 15–21 DIV neurons and not sensitive to La^{3+}. However, after treatment with Tg, addition of external Ca^{2+} induces a very large rise in $[Ca^{2+}]_{cyt}$ in 4–8 DIV neurons that is reversed largely by the classic SOCE antagonist La^{3+}, thus reflecting SOCE activation. In contrast, Ca^{2+} addition to 15–21 DIV neurons treated with Tg induced a much smaller rise than in 4–8 DIV neurons that was also partially sensitive to La^{3+} but only slightly larger than the rise recorded in neurons not treated with Tg (Fig. 1A, B). Fig. 1C shows the quantification of SOCE in 4–8 DIV and 15–21 DIV neurons after removal of the rise in $[Ca^{2+}]_{cyt}$ in cells not treated with Tg. In other words Fig. 1C shows the rise in $[Ca^{2+}]_{cyt}$ elicited by empting of intracellular Ca^{2+} stores and sensitive to La^{3+}. The results indicate that SOCE is much larger in 4–8 DIV neurons than in 15–21 DIV neurons suggesting that *in vitro* aging is associated to downregulation of SOCE in rat hippocampal neurons.

3.2. In vitro aging is associated to downregulation of Stim1 and Orai1

Orai1 and Stim1 are the most important molecular players involved in SOCE. We have investigated whether these molecular players are expressed in short-term and long-term cultures of rat hippocampal neurons. Fig. 2A shows immunofluorescence images of rat hippocampal neurons cultured for several DIV corresponding to Orai1 and Stim1 expression. Data suggest that expression of both Orai1 and Stim1 decreases with culture time. Quantitative analysis of optical density of immunofluorescence images indicates that expression of both molecular players decreases significantly in 15–21 DIV cultures relative to 4–8 DIV cultures (Fig. 2A, B). However, immunostaining of β III tubulin, a neuronal marker whose expression does not change with aging, is similar in young and aged neurons (Fig. 2C).

3.3. In vitro aging increases Ca^{2+} store content and caffeine-induced Ca^{2+} release in rat hippocampal neurons

Ca^{2+} store content was tested in rat hippocampal neurons by monitoring the rise in $[Ca^{2+}]_{cyt}$ induced by the Ca^{2+} ionophore ionomycin added in medium devoid of external Ca^{2+}. We found that ionomycin-induced rises in $[Ca^{2+}]_{cyt}$ in hippocampal neurons were small in 4–8 DIV cultures (Fig. 3A) and increased significantly in 15–21 DIV cultures (Fig. 3B). In addition, resting levels of $[Ca^{2+}]_{cyt}$ recorded before removal of extracellular Ca^{2+} were also lower in 4–8 DIV neurons than in 15–21 DIV neurons (Fig. 3A, B). For comparisons, we have calculated the area under the curves (Fig. 3C) as well as the maximum rise in $[Ca^{2+}]_{cyt}$ from the basal line (Fig. 3D). Results show that both parameters reflecting Ca^{2+} stores content are significantly larger in 15–21 DIV neurons than in 4–8 DIV neurons, thus suggesting that *in vitro* aging in rat hippocampal neurons is associated to enhanced resting $[Ca^{2+}]_{cyt}$ as previously reported [4] and increased Ca^{2+} stores content.

Ca^{2+} release activated by ryanodine receptors was tested next in short and long-term cultured hippocampal neurons. For this end, the effects of caffeine on $[Ca^{2+}]_{cyt}$ were investigated in 4–8 DIV and 15–21 DIV cultures. For these experiments, caffeine was added in nominally free Ca^{2+} (without adding EGTA). Media in these conditions contains about 50 μM Ca^{2+}, which is not relevant for Ca^{2+} influx but is

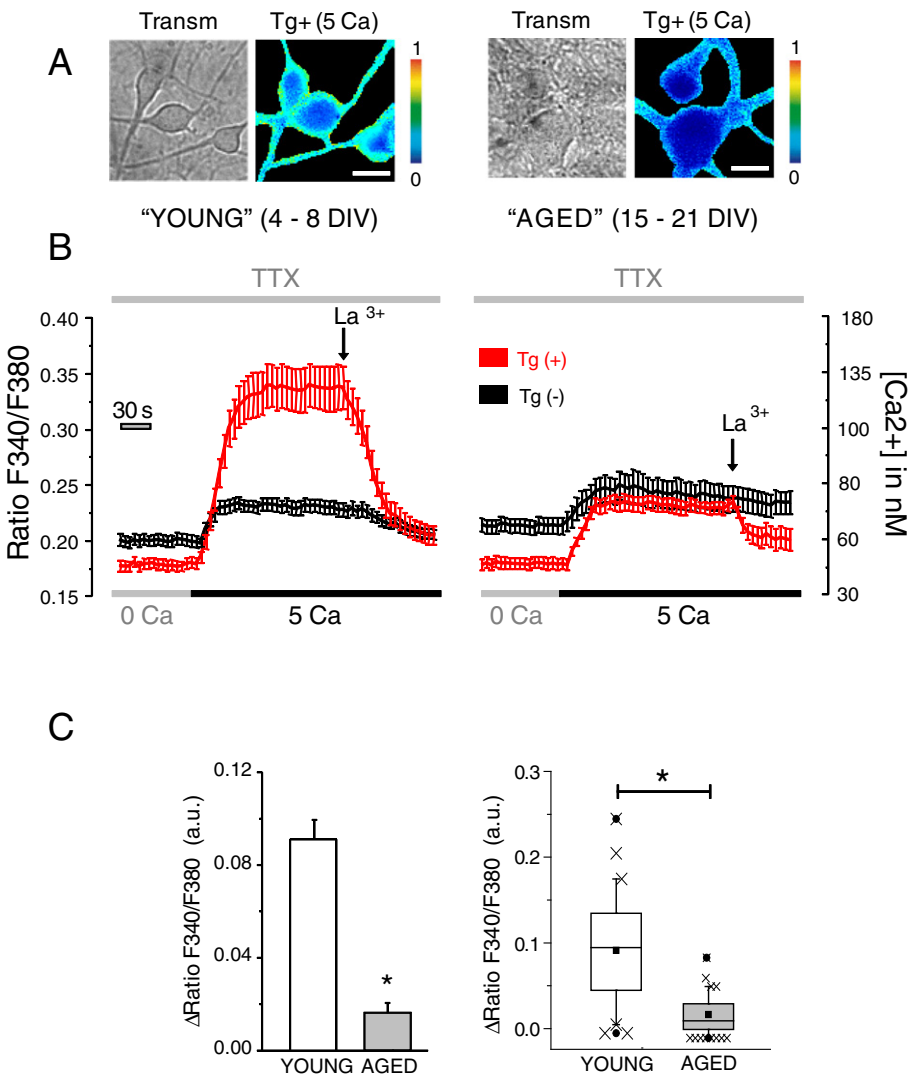

Fig. 1. *In vitro* aging decreases store-operated Ca^{2+} entry (SOCE) in rat hippocampal neurons. Store-operated Ca^{2+} entry was tested in hippocampal neurons from short-term (4–8 DIV) and long-term (15–21 DIV) cultures. Cells were loaded with fura2, treated with thapsigargin (Tg, 1 μM) in external Ca^{2+} free medium for 15 min and subjected to fluorescence Ca^{2+} imaging. Cells were perfused with external medium containing extracellular Ca^{2+} 5 mM in the presence of TTX (500 nM). A. Pictures show transmission (Transm) images as well as calcium images (Ratio F340/F380) of the same neurons coded in pseudocolor after addition of Ca^{2+} 5 mM young and aged cultures. Pseudocolor scales for Ratio F340/F380 are shown at right. Bar corresponds to 10 μm. B. Representative Ratio F340/F380 recordings (mean ± SEM) from 4 to 5 cells in control cells not treated with Tg (Tg−, black recordings) o treated with Tg (Tg+, red recordings). Cytosolic $[Ca^{2+}]$ scale is shown at right. Addition of La^{3+} inhibits SOCE. C. Left bars are average (mean ± SEM) values of ΔRatio F340/F380 reflecting SOCE in young and aged neurons. The rises in $[Ca^{2+}]_{cyt}$ in cells not treated with thapsigargin (black recordings) were subtracted for rises in Tg treated cells to estimate the size of SOCE. Right bars correspond to box plots of the same data. Data are from 49 and 37 individual cells studied in 3 (young) and 4 (aged) independent experiments. *$p < 0.05$.

permissive for Ca^{2+}-induced Ca^{2+} release. We found that caffeine increased $[Ca^{2+}]_{cyt}$ in 4–8 DIV and 15–21 DIV neurons (Fig. 3E, F). In addition, Ca^{2+} responses to caffeine were seemingly larger in 15–21 DIV neurons than in 4–8 DIV cultures. Ca^{2+} responses to agonists in primary cultures are always heterogeneous, often with large differences from cell to cell. As reported previously [4], to quantify Ca^{2+} responses of the whole cell population in cells populations containing a mix of responsive and unresponsive cells we computed the average change in fluorescence ratio (ΔRatio F340/F380) in the responsive cell population (Fig. 3G) and the fraction of responsive cells (Fig. 3H). Then we calculate the product of both parameters, a value that reflects properly the response of the whole cell population (Fig. 3I). Results show that Ca^{2+} release induced by caffeine in the whole cell population is significantly larger in 15–21 DIV neurons than in 4–8 DIV neurons. Thus, suggesting that *in vitro* aging is associated to enhance caffeine-induced release of Ca^{2+} in rat hippocampal neurons.

3.4. In vitro aging increases Ca^{2+} release induced by ACh rat hippocampal neurons

ACh is an important agonist for hippocampal neurons. We also investigated effects of *in vitro* aging on Ca^{2+} responses induced by acetylcholine (ACh). Fig. 4 shows representative pseudocolor images (Fig. 4A, B) and representative $[Ca^{2+}]_{cyt}$ recordings obtained in 4–8 DIV and 15–21 DIV neurons stimulated with ACh. Cytosolic Ca^{2+} responses were larger in 15–21 DIV neurons than in 4–8 DIV cultures (Fig. 4A, B). However, differences were seemingly due to both changes in the size of $[Ca^{2+}]_{cyt}$ rises in responsive cells (Fig. 4C) and the relative number (fraction) of responsive cells (Fig. 4D). As a whole, Ca^{2+} responses to ACh are larger in 15–21 DIV neurons relative to 4–8 DIV cultures (Fig. 4E).

Ca^{2+} responses to ACh may be due to both Ca^{2+} release and Ca^{2+} entry. To investigate the influence of *in vitro* aging on Ca^{2+} release

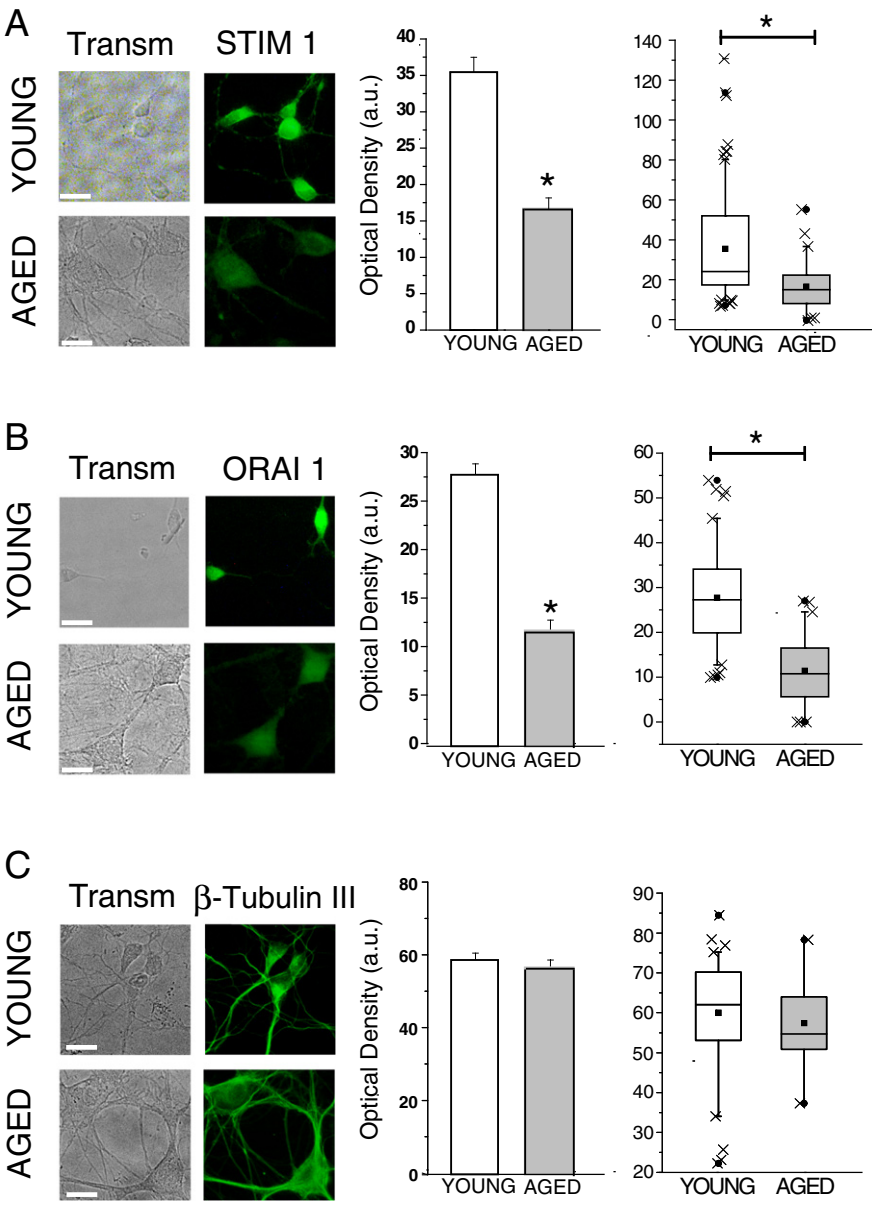

Fig. 2. *In vitro* aging is associated to decreased expression of Stim1 and Orai1. Short-term and long-term cultures of hippocampal neurons were fixed and expression of Stim1 and Orai1 was tested by immunofluorescence. A. Representative images of bright field (Transm) and Stim1 immunofluorescence from 3 DIV and 21 DIV rat hippocampal neurons. Scale bar is 10 μm. Bars show optical density values and box plot data corresponding to 149 and 49 cells, respectively *$p < 0.05$. B. Representative images of bright field (Transm) and Orai1 immunofluorescence from 3 DIV and 21 DIV rat hippocampal neurons. Scale bar is 10 μm. Bars show optical density values and box plot data corresponding to 84 and 52 cells, respectively *$p < 0.05$. C. Representative images of bright field (Transm) and βIII tubulin immunofluorescence from 3 DIV and 21 DIV rat hippocampal neurons. Scale bar is 10 μm. Bars show optical density values and box plot data corresponding to 78 and 18 cells, respectively.

induced by ACh we tested the effects of this agonist on $[Ca^{2+}]_{cyt}$ in the absence of extracellular Ca^{2+}. ACh increased $[Ca^{2+}]_{cyt}$ in the absence of extracellular Ca^{2+} indicating release of Ca^{2+} from intracellular stores. This effect was abolished in the presence of atropine, an antagonist of muscarinic receptors, thus indicating that Ach induces Ca^{2+} release upon activation of muscarinic receptor (data not shown). We found that ACh-induced Ca^{2+} release is larger in 15–21 DIV cultures than in 4–8 DIV cultures as shown in Fig. 4F, G. Interestingly, despite that Ca^{2+} store content is larger in the *in vitro* aged neurons, rises in $[Ca^{2+}]_{cyt}$ induced by Ca^{2+} release evoked by ACh in responsive cells are similar in 4–8 DIV and 15–21 DIV cultures (Fig. 4H) suggesting increased buffering in 15–21 DIV neurons.

The relative number (fraction) of ACh responsive cells was larger in 15–21 DIV neurons than 4–8 DIV neurons (Fig. 4I). Specifically, whereas only 35% of all neurons in short-term cultures are responsive to ACh in Ca^{2+}-free medium, almost 80% of all long-term cultured neurons released Ca^{2+} in response to ACh. Due to this difference, the product of the ΔCa^{2+} in responsive neurons by the fraction of responsive cells is larger in 15–21 DIV neurons (Fig. 4J). Taken together, these data suggest differences in the way that young and aged neurons handle Ca^{2+} release induced by physiological agonists. We tested next whether ER mitochondria coupling could be involved in the differential handling.

3.5. *In vitro aging increases Ca^{2+} transfer from ER to mitochondria*

We tested next the effects of preventing mitochondrial Ca^{2+} uptake using the mitochondrial uncoupler FCCP on the rises in $[Ca^{2+}]_{cyt}$ induced by Ca^{2+} release evoked by ACh in 4–8 DIV and 15–21 DIV cultures (Fig. 5). We found that ACh-induced $[Ca^{2+}]_{cyt}$ increases in Ca^{2+} free medium are dramatically enhanced in 15–21 DIV neurons

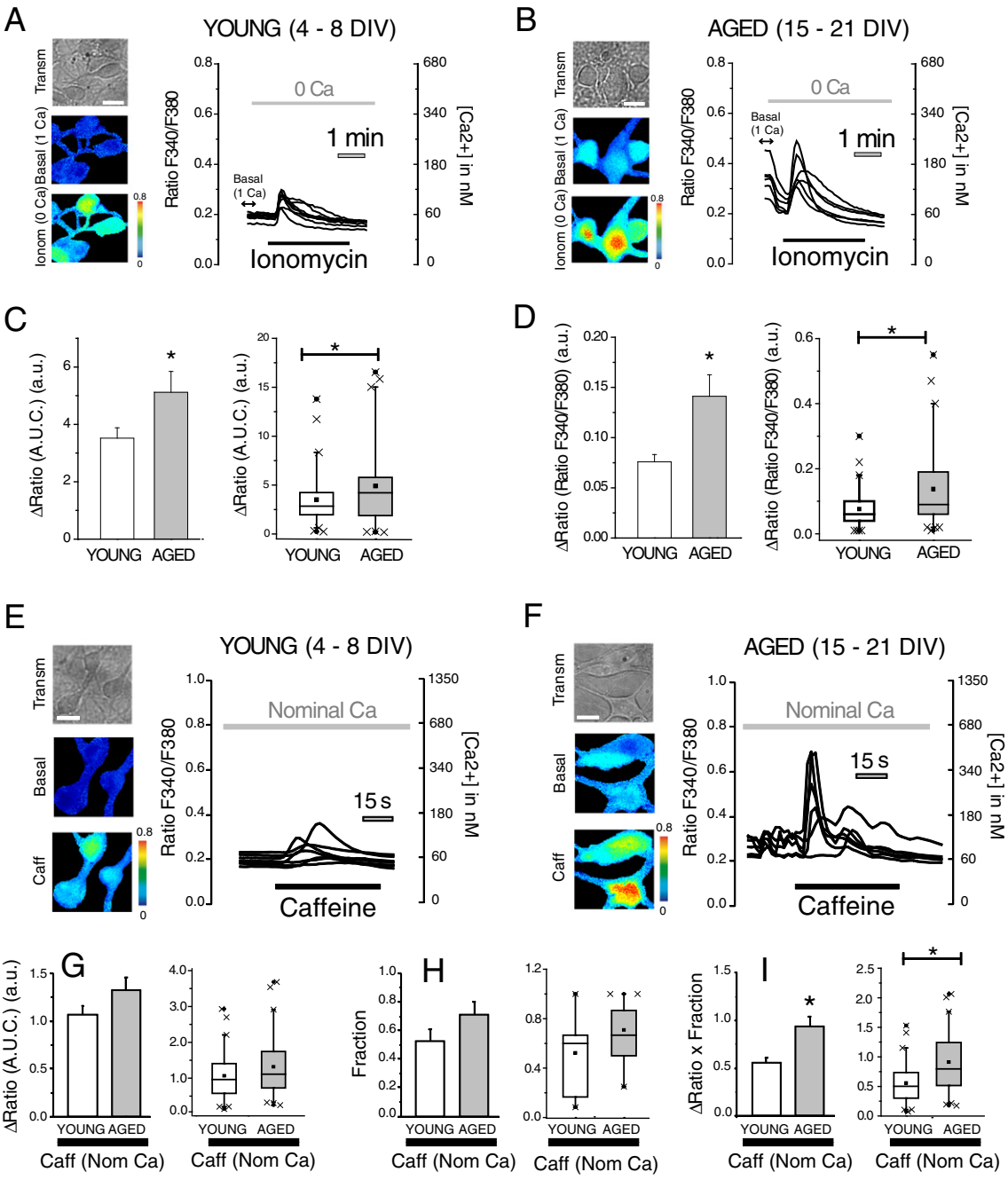

Fig. 3. *In vitro* aging increases Ca^{2+} store content and caffeine-induced Ca^{2+} release in rat hippocampal neurons. Hippocampal neurons were loaded with fura2 and subjected to fluorescence imaging for monitoring Ca^{2+} store content and Ca^{2+} release. Cells were perfused with ionomycin 400 nM (Ionom) in external medium devoid of Ca^{2+} (0 Ca). Pictures show transmission (Transm) and pseudocolor images of fluorescence ratios in basal conditions - Basal (1 Ca) - and after ionomycin - Ionom (0 Ca) - in short-term (A, 4–8 DIV) and long-term (B, 15–21 DIV) cultured neurons. Pseudocolor scales shown at right. Bar represents 10 μm. Traces are representative recordings of fluorescence ratios in individual neurons identified by their morphology. Cytosolic $[Ca^{2+}]$ scale is shown at right. Bars are average (mean ± SEM) areas under traces (C) or maximum rises in ratios (D) and corresponding box plot data in 4–8 DIV and 15–21 DIV cultures ($n = 46$, 53 individual cells from 4 independent cultures (*$p < 0.05$). Box plots of the same data are shown Ca^{2+} release induced by caffeine was tested in 4–8 DIV (E) and 15–21 DIV cultures (F). Pictures show transmission images (Transm) and pseudocolor images of fluorescence ratios in basal conditions (Basal) and after caffeine 20 mM. Pseudocolor scales shown at right. Bar corresponds to 10 μm. Traces are representative recordings of fluorescence ratios of individual neurons identified by their morphology. Bars correspond to the average (mean ± SEM) areas under traces in caffeine-responsive cells (G), the fraction of cells responding to caffeine (H) or the product of both parameters (I) and corresponding box plot data. $n = 101$ and 55 cells from 4 independent experiments, respectively (*$p < 0.05$).

treated previously with FCCP. However, prevention of mitochondrial Ca^{2+} uptake with FCCP has only a minor effect on the response to ACh in 4–8 DIV neurons (Fig. 5A–D). In other words, the effects of FCCP on the rise in $[Ca^{2+}]_{cyt}$ induced by ACh were much larger in 15–21 DIV neurons than in 4–8 DIV neurons (Fig. 5E). In addition, FCCP has no effect on the relative number (fraction) of cells responsive to A-Ch. These results suggest that Ca^{2+} released from the ER after IP_3 receptor activation is barely seen by mitochondria in 4–8 DIV neurons. However, in 15–21 DIV neurons, a large fraction of Ca^{2+} released from the ER is efficiently transferred to surrounding mitochondria.

To support further the above view we have monitored directly the rise in mitochondrial Ca^{2+} concentration ($[Ca^{2+}]_{mit}$) elicited by Ca^{2+} release induced by ACh in medium devoid of external Ca^{2+} (Fig. 6). For this end, hippocampal neurons were transfected with a mitochondria-targeted

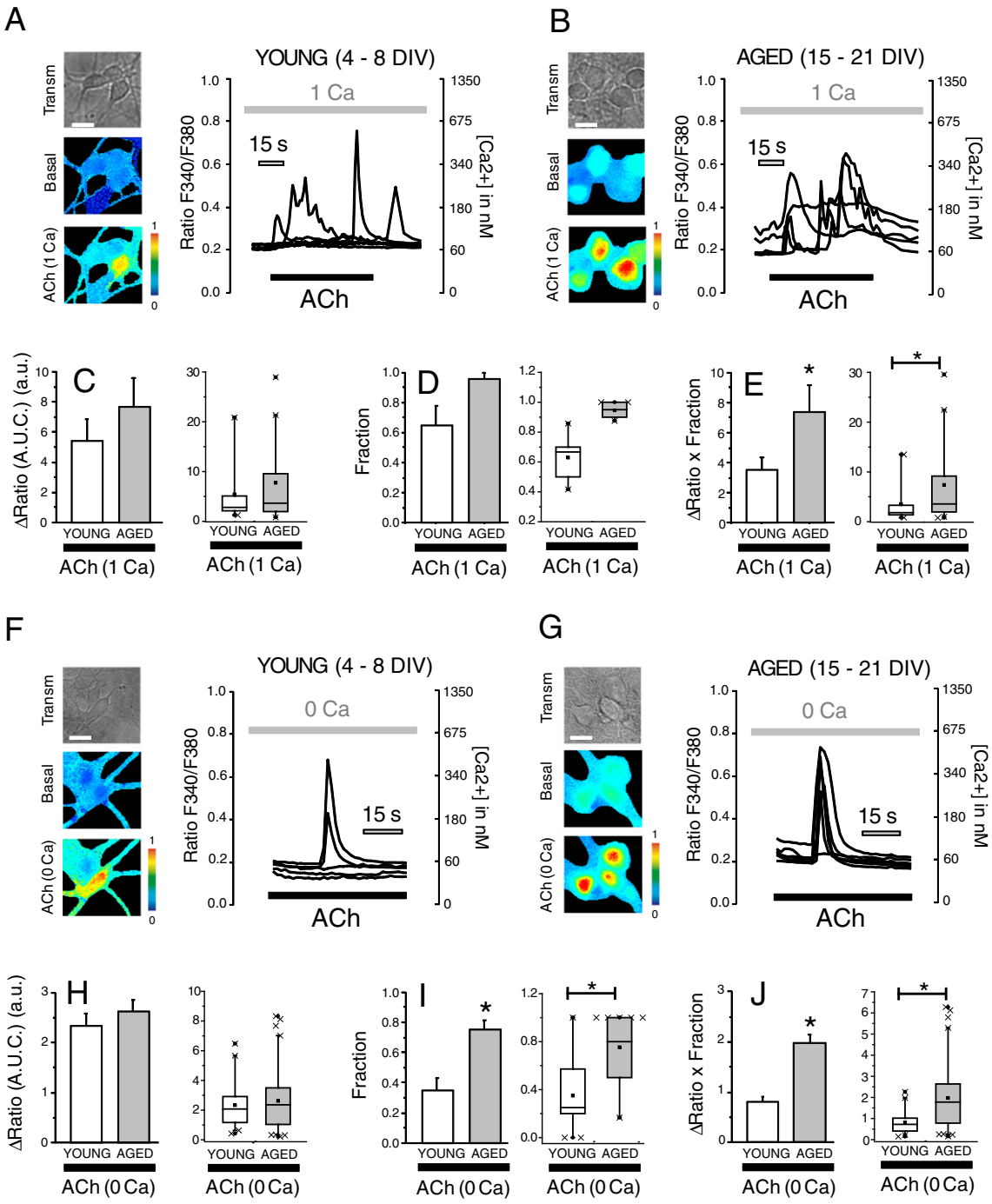

Fig. 4. *In vitro* aging increases Ca^{2+} responses to acetylcholine in rat hippocampal neurons. Hippocampal neurons were loaded with fura2 and subjected to fluorescence imaging for monitoring the effects of ACh in short-term (A, 4–8 DIV) and long-term (B, 15–21 DIV) cultured neurons. Cells were stimulated with acetylcholine 100 μM in Ca^{2+}-containing medium. Pictures show transmission images (Transm) and pseudocolor images of fluorescence ratios taken before (Basal) and after acetylcholine - ACh (1 Ca). Pseudocolor scale shown at right. Bar corresponds to 10 μm. Traces are representative recordings of fluorescence ratios of individual neurons identified by their morphology in 4–8 DIV and 15–21 DIV cultures. Bars correspond to the average (mean ± SEM) areas under traces in ACh-responsive cells (C), the fraction of responsive cells (D) or the product of both parameters (E) and corresponding box plot data. $n = 25$ and 22 cells from 3 independent experiments (*$p < 0.05$). Ca^{2+} release induced by ACh in Ca^{2+}-free medium was monitored in short-term (F, 4–8 DIV) and long-term (G, 15–21 DIV) cultured neurons. Pictures show transmission images (Transm) and pseudocolor images of fluorescence ratios taken before (Basal) and after acetylcholine - ACh (0 Ca). Pseudocolor scale shown at right. Bar represents 10 μm. Traces are representative recordings of fluorescence ratios of individual neurons identified by their morphology in 4–8 DIV and 15–21 DIV cultures. Bars correspond to the average (mean ± SEM) areas under traces of responsive cells (H), the fraction of responsive cells (I) and the product of both parameters (J) and corresponding box plot data. n = 101 and 109 cells from 6 and 8 independent experiments (*$p < 0.05$).

aequorin and subjected to bioluminescence imaging for monitoring of $[Ca^{2+}]_{mit}$ in transfected neurons. Transfection efficiency was similar (15 ± 5%) for both short-term and long-term cultured neurons. Transfected neurons in the microscopic field were selected by their GFP fluorescence and subjected to bioluminescence imaging. Fig. 6A shows representative fluorescence and bioluminescence images of transfected neurons and representative traces of the rises in $[Ca^{2+}]_{mit}$ induced by ACh in Ca^{2+} free medium. Results show that both the rises in $[Ca^{2+}]_{mit}$ induced by ACh and the relative number of responsive cells (fraction) are significantly larger in 15–21 DIV neurons than in 4–8 DIV neurons

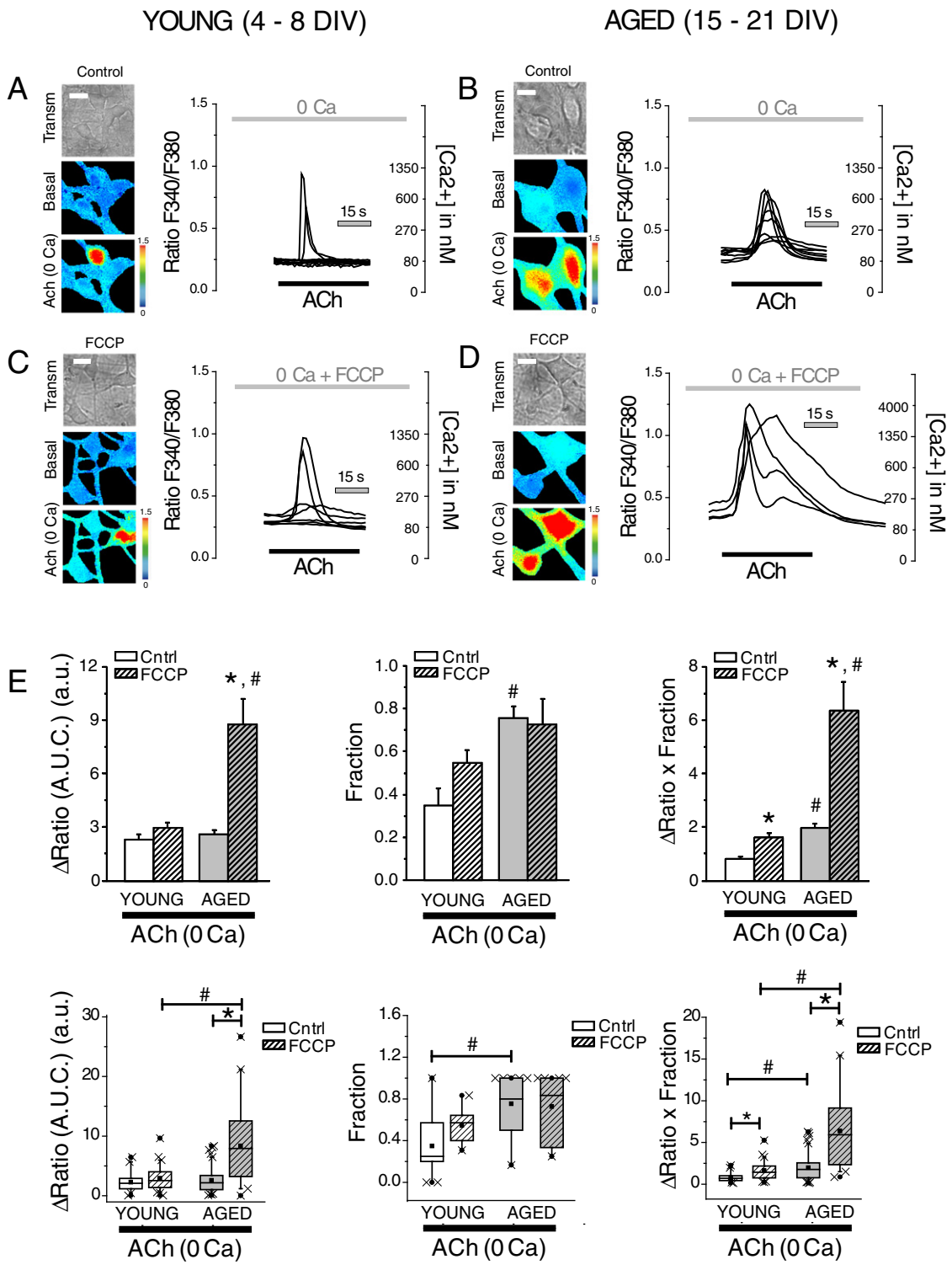

Fig. 5. Most Ca^{2+} released from the ER is taken up by mitochondria in 15–21 DIV neurons but not in 4–8 DIV neurons. Hippocampal neurons were loaded with fura2 and subjected to fluorescence imaging for monitoring the effects of the mitochondrial uncoupler FCCP on the rise in $[Ca^{2+}]_{cyt}$ evoked by ACh-induced Ca^{2+} release. Pictures show transmission images (Transm) and pseudocolor images of fluorescence ratios taken before (Basal) and after acetylcholine - ACh (0 Ca) - in 4–8 DIV (A, 4–8 DIV) and 15–21 DIV (B, 15–21 DIV) cultured neurons. Traces are representative recordings of fluorescence ratios of individual neurons identified by their morphology in 4–8 DIV and 15–21 DIV cultures in the absence (A,B) or the presence of FCCP (C,D). E. Bars correspond to the average (mean ± SEM) areas under traces in responsive cells (left panel), the fraction of responsive cells (middle panel) or the product of both parameters (right panel) and corresponding box plot data. n = 101, 84, 109 and 34 cells from 4 to 8 independent experiments (*p < 0.05 *vs.* control; #p < 0.05 *vs.* 4–8 DIV cultures).

(Fig. 6B). Consistently with the FCCP results shown above, bioluminescence imaging of $[Ca^{2+}]_{mit}$ indicate that mitochondria from 4 to 8 DIV neurons are essentially blind to Ca^{2+} release induced by ACh. In contrast, in 15–21 DIV neurons, a fraction of mitochondria become functionally coupled to Ca^{2+} stores consistently with efficient Ca^{2+} transfer from the ER to mitochondria Ca^{2+}.

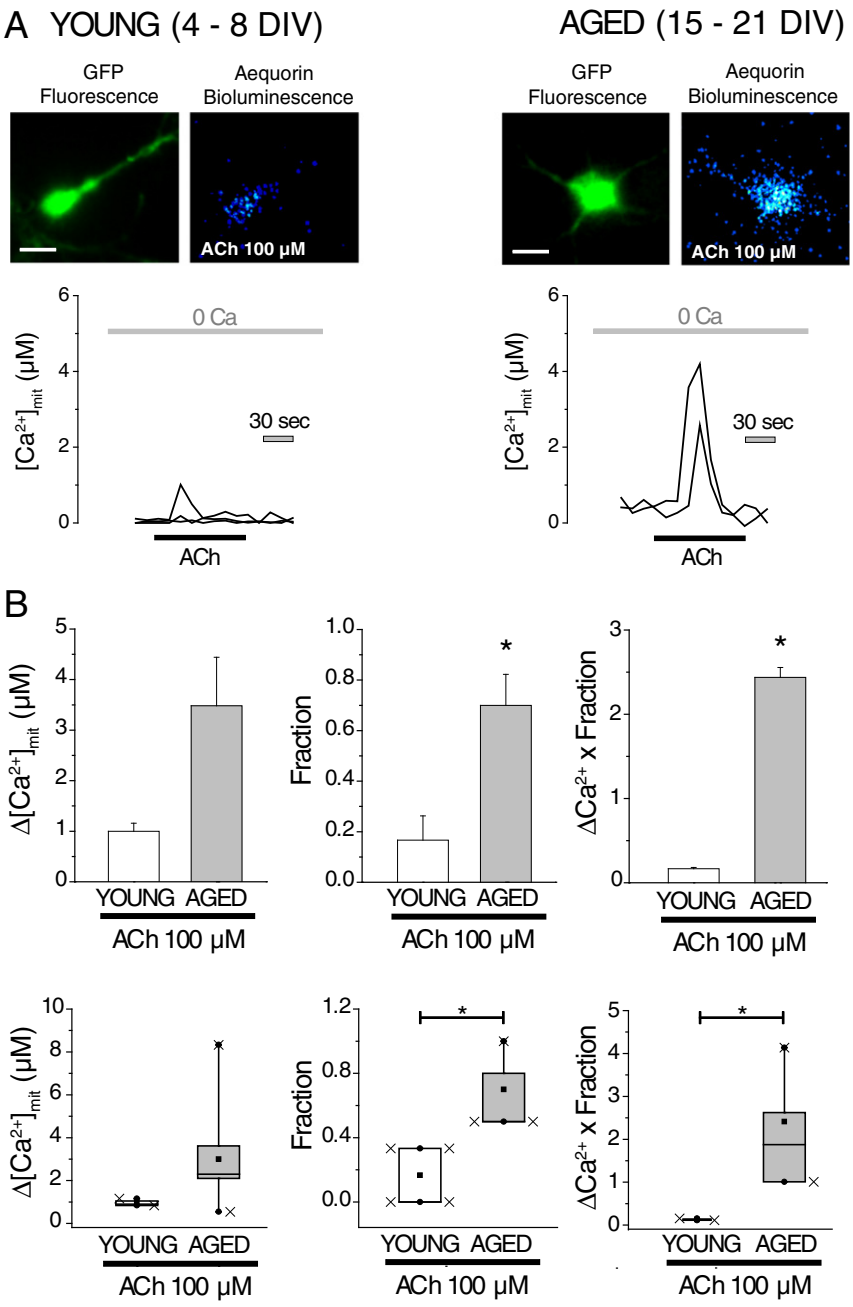

Fig. 6. Mitochondrial Ca^{2+} uptake induced by Ca^{2+} release in short-term and long-term cultured hippocampal neurons. A. Hippocampal neurons were transfected with mitochondria-targeted, GFP aequorin and subjected to bioluminescence imaging for monitoring mitochondrial Ca^{2+} uptake. Pictures show fluorescence (GFP fluorescence) and bioluminescence (Aequorin Bioluminescence) images of short-term (4–8 DIV) and long-term (15–21 DIV) cultured hippocampal neurons. Photonic emissions representing mitochondrial Ca^{2+} uptake were obtained during perfusion with ACh 100 µM in Ca^{2+} free medium (0 Ca). Traces are representative recordings of the rises in mitochondrial Ca^{2+} concentration ($[Ca^{2+}]_{mit}$) induced by Ca^{2+} release evoked by ACh 100 µM in Ca^{2+}-free medium. B. Bars correspond to the average (mean ± SEM) rises in $[Ca^{2+}]_{mit}$ in responsive cells (left panel), the fraction of responsive cells (middle panel) and the product of both parameters (right panel) and corresponding box plot data. $n = 13$ and 15 cells from 4 independent experiments (*$p < 0.05$).

3.6. The mitochondrial Ca^{2+} uniporter is upregulated in 15–21 DIV rat hippocampal neurons

One of the most important players involved in mitochondrial Ca^{2+} uptake is the recently cloned mitochondrial Ca^{2+} uniporter (MCU) [32,33]. We have tested changes in relative expression of MCU in hippocampal neurons along with time in culture using specific immunofluorescence and optical density quantification in 4–8 DIV and 15–21 DIV cultures. Fig. 7A shows immunofluorescence images of rat hippocampal neurons cultured for several DIV corresponding to MCU expression. Data suggest that MCU expression increases with culture time. Quantitative analysis of optical density of immunofluorescence images indicates that expression of MCU in individual neurons is increased significantly in 15–21 DIV cultures relative to 4–8 DIV cultures (Fig. 7B). Notice that optical density of immunofluorescence images of βIII tubulin, a neural marker whose expression does not change, is similar in 4–8 DIV cultures than in 15–21 DIV cultures (Fig. 2C).

3.7. In vitro aging is associated to mitochondrial depolarization and decreased mitochondrial Ca^{2+} uptake in permeabilised neurons

Finally, we have also investigated mitochondrial Ca^{2+} uptake in permeabilised neurons and $\Delta\Psi$, the driving force for mitochondrial Ca^{2+} uptake in 4–8 DIV and 15–21 DIV hippocampal neurons. For this

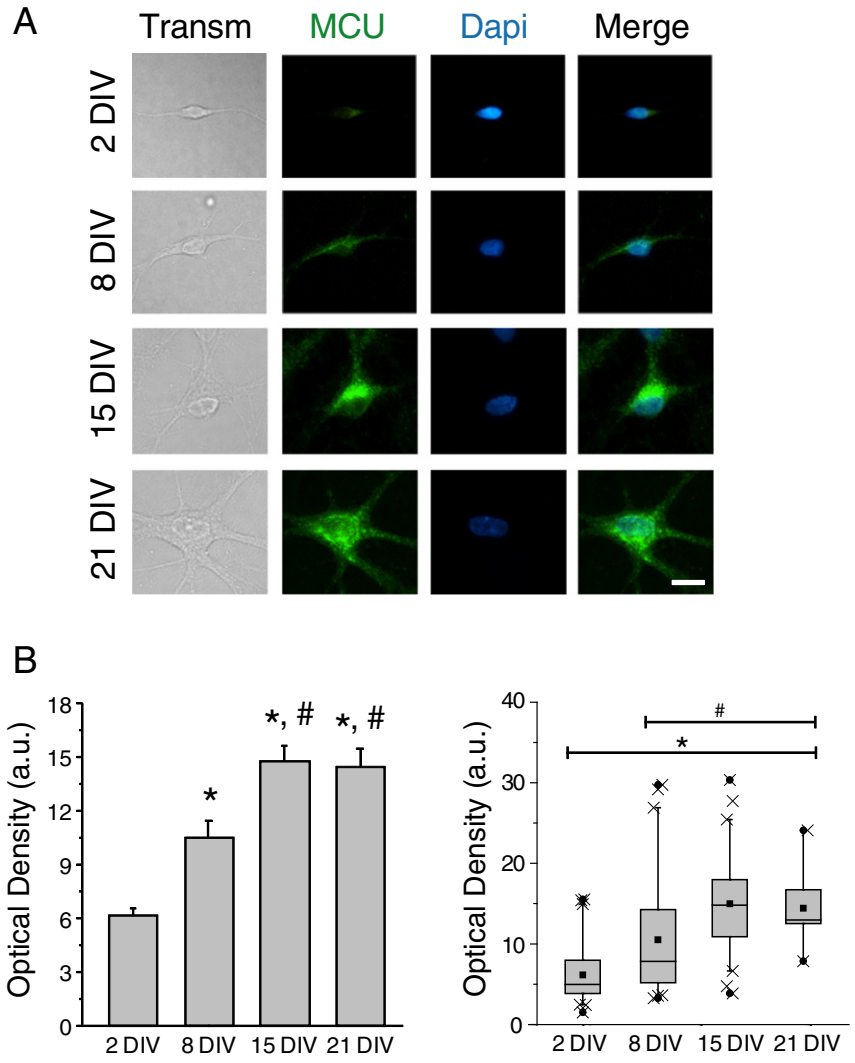

Fig. 7. Aging increases expression of the mitochondrial Ca^{2+} uniporter in rat hippocampal neurons. Hippocampal neurons were cultured for 2, 8, 15 and 21 DIV and expression of MCU was tested using immunofluorescence and a specific antibody. A. Representative bright field (Transm), immunofluorescence images of the mitochondrial calcium uniporter (MCU), nuclei (DAPI) and merge images taken in rat hippocampal neurons cultured for 2, 8, 15 and 21 DIV. Scale bar is 10 μm and applies to all frames. B. Quantitative analysis of immunofluorescence intensity levels (Optical Density in arbitrary units) for MCU. Bars represent mean ± SEM from 57, 51, 45 and 19 cells from 3 independent experiments and corresponding box plot data. *$p < 0.05$ *vs.* 2 DIV; #$p < 0.05$ *vs.* 8 DIV.

end, transfected neurons expressing a low-affinity, mitochondria-targeted GFP aequorin, were permeabilised in with digitonin solved in internal medium containing very low Ca^{2+} concentration (200 nM) to mimic $[Ca^{2+}]_{cyt}$. Then neurons were stimulated with internal medium containing 10 μM Ca^{2+}, a concentration required for mitochondrial Ca^{2+} uptake [17,18]. Fig. 8A, B shows that both 4–8 DIV and 15–21 DIV neurons undergo rises in mitochondrial Ca^{2+} uptake when exposed to 10 μM Ca^{2+}. Interestingly, the rise in $[Ca^{2+}]_{mit}$ was significantly larger in 4–8 DIV neurons than in 15–21 DIV neurons. These results are unexpected as 15–21 DIV display enhanced expression of the MCU. However, as stated above, we and others have shown that *in vitro* aging is associated to mitochondria depolarization [4]. We confirmed this view by monitoring TMRM staining in 4–8 DIV and 15–21 DIV neurons. TMRM accumulates inside mitochondria according to $\Delta\Psi$. Fig. 7C shows representative images of TMRM fluorescence confirming that TMRM accumulates largely in mitochondria of 4–8 DIV but only poorly in mitochondria from 15 to 21 DIV cultures. These results indicate that long-term cultures of rat hippocampal neurons show depolarized mitochondria and decreased global mitochondrial Ca^{2+} uptake when exposed to similar concentrations of Ca^{2+}.

4. Discussion

Here we show that long-term culture of rat hippocampal neurons, a model of *in vitro* aging, is associated to downregulation of SOCE and increased transfer of Ca^{2+} from ER to mitochondria (ER-mitochondrial Ca^{2+} cross talk). These results have been obtained in an *in vitro* model of aging and, therefore, may not reflect entirely the physiological aging of the brain. However, in support of the findings, it has been previously shown that long-term cultured rat hippocampal neurons acquire important hallmarks of neuronal aging *in vivo* including ROS accumulation, lipofuscin granules, heterochromatic foci, activation of pJNK and p53/p21 pathways and loss of cholesterol among others [1,3,4]. Therefore, the remodeling of subcellular Ca^{2+} in aging neurons reported here may contribute to cognitive decline and the susceptibility to neuron cell death that is characteristic of the elderly.

SOCE is a widespread calcium entry pathway involved in different physiological functions in multiple types of cells [7]. In hippocampal neurons, the presence and functions of SOCE have remained elusive. Recent evidence indicates, however, that SOCE is required for the sustained activation of calmodulin-kinase II (CamKII) and the stabilization of mature

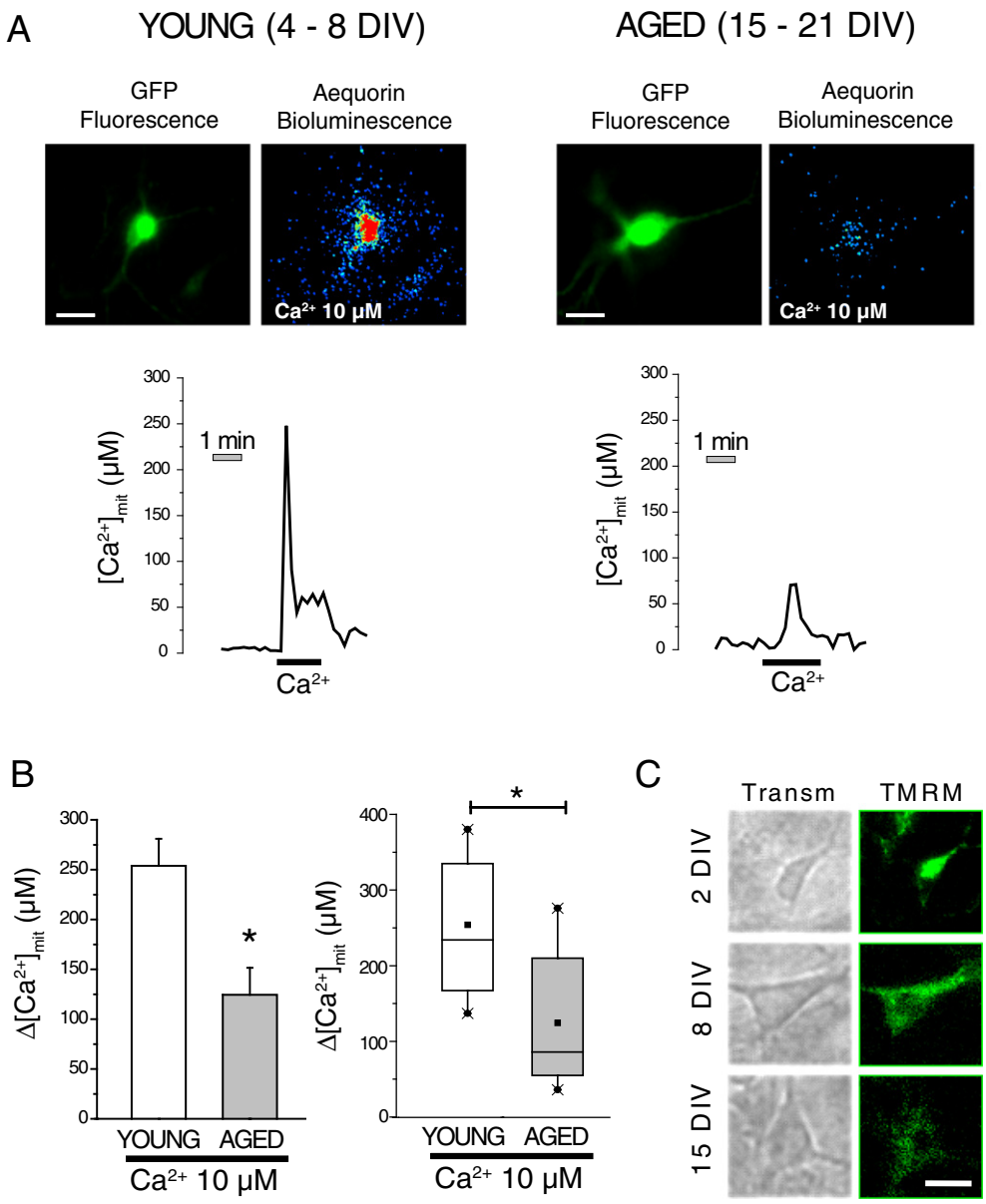

Fig. 8. *In vitro* aging is associated to mitochondria depolarization and decreased mitochondrial Ca^{2+} uptake in permeabilised neurons. A. Cells were transfected with mutated, mitochondria-targeted, GFP aequorin and subjected to bioluminescence imaging for monitoring mitochondrial Ca^{2+} uptake induced by 10 µM Ca^{2+} in permeabilised cells. Pictures show fluorescence (GFP Fluorescence) and bioluminescence (Aequorin Bioluminescence) images in "young" (4–8 DIV) and "aged" (15–21 DIV) cultured hippocampal neurons. Traces are representative recordings of rises in mitochondrial Ca^{2+} concentration ($[Ca^{2+}]_{mit}$) induced by 10 µM Ca^{2+} in 4–8 DIV and 15–21 DIV cultures. B. Bars correspond to averaged (mean ± SEM) rises in $[Ca^{2+}]_{mit}$ in 4–8 DIV and 15–21 DIV cultures and corresponding box plot data. Data are from 10 and 11 cells from 5 independent experiments (*$p < 0.05$). C. Hippocampal neurons were cultured for 2, 7 and 15 DIV. Then cells were washed and incubated with the mitochondrial potential probe TMRM 10 nM before fluorescence imaging. Images are representative bright field (Transm) and fluorescence images. Bar in pictures represents 10 µm. Data are representative of three independent experiments.

mushroom spines [34]. Mushroom spines between excitatory neurons are considered stable memory spines that make functionally stronger synapsis responsible of memory storage [35]. Accordingly, downregulation of SOCE in aging neurons could compromise mushroom spines stability and cognitive performance. It is tempting to speculate that SOCE downregulation with aging may contribute to impaired stability of mushroom spines leading to reduced ability for learning and memory storage. Interestingly, a similar mechanism has been recently put forward to explain exacerbated cognitive decline associated to AD [6].

Molecular players involved in SOCE in hippocampal neurons are not completely understood. It has been proposed that, at variance with most cell types, SOCE in hippocampal neurons is driven by Stim2, rather than Stim1 [12]. However, recent results suggest that Stim1 mainly activates SOCE, whereas Stim2 regulates resting Ca^{2+} levels in the ER and Ca^{2+} leakage with the additional involvement of Stim1 [13]. We show here that Stim1 and Orai1 are downregulated in aged neurons *in vitro* while expression of βIII tubulin, a neural marker that does not change with aging, remains similar in young and aged neurons (Fig. 2C). Therefore, loss of SOCE in long-term cultured rat hippocampal neurons could be mediated at least in part by downregulation of Stim1 and Orai1. Further research is required to ascertain whether these molecular players are downregulated with aging *in vivo*.

Additional factors may contribute to SOCE downregulation in aging neurons. For example, SOCE depends on mitochondrial Ca^{2+} uptake required for preventing Ca^{2+}-dependent inactivation of store-operated channels [31,36,37]. In fact, it has been shown that mitochondrial depolarization prevents mitochondrial Ca^{2+} uptake and inhibits SOCE in different cell types [38]. Accordingly, it is possible that the mitochondrial depolarization characteristic of aged neurons may lead also to Ca^{2+}-dependent inactivation of SOC channels and SOCE downregulation in

aging. Further research is required to ascertain more precisely the mechanisms involved in SOCE downregulation in aging neurons.

The other mayor change in subcellular Ca^{2+} homeostasis in 15–21 DIV neurons is the enhanced Ca^{2+} transfer from the ER to mitochondria. Evidences in support of this view are several fold. First, direct measurements of $[Ca^{2+}]_{mit}$ in transfected neurons using mitochondria-targeted aequorin and bioluminescence imaging shows that only mitochondria from 15 to 21 DIV neurons undergo rises in $[Ca^{2+}]_{mit}$ evoked by ACh-induced Ca^{2+} release. In contrast, mitochondria from 4 to 8 DIV neurons are blind to ACh-induced Ca^{2+} release. Second, inhibition of mitochondrial Ca^{2+} uptake with FCCP enhances dramatically the rise in $[Ca^{2+}]_{cyt}$ induced by Ca^{2+} release in 15–21 DIV neurons whereas having a much lower effect in 4–8 DIV neurons. These results indicate that a large part of Ca^{2+} released from the ER is actually taken up by mitochondria in long-term cultured neurons *in vitro* but not in 4–8 DIV neurons.

Several mechanisms may contribute to the ER-mitochondria cross talking including changes in ER, mitochondria and ER-mitochondria interface. Regarding the ER, the first mechanism is the size of Ca^{2+} stores in 15–21 DIV neurons that is enhanced relative to 4–8 DIV neurons. Therefore, ACh-induced Ca^{2+} release may form Ca^{2+} microdomains large and sustained enough to promote mitochondrial Ca^{2+} uptake in surrounding mitochondria. Enhanced Ca^{2+} store content could be mediated by the larger resting $[Ca^{2+}]_{cyt}$ observed in 15–21 DIV neurons reported previously [4] and confirmed here which favours SERCA activity. Enhanced resting $[Ca^{2+}]_{cyt}$ in aging neurons could be mediated by age-related loss of endogenous Ca^{2+} buffers such as calbindinD28k as recently reported [39,40]. In addition to Ca^{2+} store content, Ca^{2+} release is also enhanced in 15–21 DIV neurons compared to 4–8 DIV cultures as shown by the rises in $[Ca^{2+}]_{cyt}$ induced by caffeine and ACh in Ca^{2+} free medium. These effects could be mediated by age-related changes in expression and/or activity of Ca^{2+} release channels [41]. Regarding mitochondria, increased Ca^{2+} transfer from ER to mitochondria could also be facilitated by enhanced expression of the MCU, the Ca^{2+} channel responsible for mitochondrial Ca^{2+} uptake. Our present results using immunofluorescence against MCU in morphologically identified hippocampal neurons support this possibility. As a caution note, as stated above, results on MCU expression in aging should be confirmed in aged rats as well.

In spite of increased expression of MCU in 15–21 DIV, permeabilised neurons show decreased mitochondrial Ca^{2+} uptake when challenged with 10 μM Ca^{2+} which is consistent with the loss of mitochondrial potential observed in "aged" neurons. To reconcile these seemingly contradictory (paradoxical) results we must take into account that, as previously reported, functional coupling between ER and mitochondria is mediated by the so-called mitochondria associated ER membranes (MAMs), a specialized domain of close contact sites between the ER and mitochondria involved in maintaining a dynamic cross-talk between the two organelles [22,23]. This domain enables formation of high Ca^{2+} microdomains restricted in space and time that, together with enhanced MCU expression, would explain increased transfer of Ca^{2+} from ER to mitochondria in aging in the face of mitochondrial depolarization. In fact, it could be hypothesized that enhanced ER-mitochondria cross-talking in aging is meant to compensate the loss of mitochondrial potential in order to maintain the signal. Further research is required to ascertain the molecular basis for enhanced ER-mitochondrial coupling in aging neurons.

ER-mitochondrial Ca^{2+} cross talk may have important physiological consequences for the aging neuron, particularly related to energy decay and susceptibility to neuron cell death in the elderly. For example, as mentioned above, a Ca^{2+} leak from ER to mitochondria is required to sustain the Krebs cycle, oxidative phosphorylation and ATP synthesis [24]. In the absence of such a flow, Krebs cycle slows down, electron transfer and ATP/AMP ratio decrease, thus leading to activation of AMP kinase (AMPK) and macro-autophagia. This pathway is intended to provide energy to metabolically compromised neurons [24] by providing a constant flow of Ca^{2+} from ER to mitochondria that is required by the Krebs cycle to keep rolling. However, if excessive Ca^{2+} is transferred, then it follows mitochondrial Ca^{2+} overload leading to apoptosis. Thus, the possible age-associated, ER-mitochondria Ca^{2+} cross talk reported here may favour energy production in aging neurons at the expense of increased risk of neuron cell death associated to mitochondrial Ca^{2+} overload during, for example, excitotoxicity and AD. Interestingly, changes in ER-mitochondria Ca^{2+} cross talk have been recently linked to AD. For example, PS2 overexpression, FAD-linked PS2 mutants and Aβ favour the interaction between ER and mitochondria, thus facilitating mitochondrial Ca^{2+} uptake and risk of neuron damage [41,42].

In summary, we report here that *in vitro* aging of rat cultured hippocampal neurons is associated to loss of SOCE and enhanced ER-mitochondria cross talking. These changes are mediated at least in part by downregulation of Stim1 and Orai1, the molecular players involved in SOCE, and changes in Ca^{2+} store content, Ca^{2+} release, upregulation of MCU and possible changes in ER-mitochondria domains in *in vitro* aged neurons. Further research is required to address whether the above remodeling of subcellular Ca^{2+} may contribute to the cognitive decline (related to SOCE loss) and increased susceptibility to neuron cell death (related to mitochondrial Ca^{2+} overload) in the elderly. The molecular basis of the above remodeling might provide novel opportunities for neuroprotection against age-related brain disorders.

Conflict of interest

None.

Transparency document

The Transparency document associated with this article can be found, in online version.

Acknowledgements

This work was supported by grants BFU2012-37146 and BFU2015-70131R from Ministry of Economy and Competitiveness (Spain) and grants VA145U13 and BIO/VA33/13 from Regional Government of Castilla y León (Spain). MCR was supported by a pre-doctoral fellowship from Regional Government of Castilla y León (Spain) and the European Social Fund.

Appendix A. Supplementary data

Supplementary data to this article can be found online at http://dx.doi.org/10.1016/j.bbamcr.2016.08.001.

References

[1] N.M. Porter, O. Thibault, V. Thibault, K.C. Chen, P.W. Landfield, Calcium channel density and hippocampal cell death with age in long-term culture, J. Neurosci. 17 (1997) 5629–5639.
[2] L.D. Brewer, O. Thibault, J. Staton, V. Thibault, J.T. Rogers, G. García-Ramos, S. Kraner, P.W. Landfield, N.M. Porter, Increased vulnerability of hippocampal neurons with age in culture: temporal association with increases in NMDA receptor current, NR2A subunit expression and recruitment of L-type calcium channels, Brain Res. 1151 (2007) 20–31.
[3] A.O. Sodero, C. Weissmann, M.D. Ledesma, C.G. Dotti, Cellular stress from excitatory neurotransmission contributes to cholesterol loss in hippocampal neurons aging in vitro, Neurobiol. Aging 32 (2011) 1043–1053.
[4] M. Calvo, S. Sanz-Blasco, E. Caballero, C. Villalobos, L. Núñez, Susceptibility to excitotoxicity in 15-21 DIV hippocampal cultures and neuroprotection by non-steroidal anti-inflammatory drugs: role of mitochondrial calcium, J. Neurochem. 132 (2015) 403–417.
[5] M. Calvo-Rodríguez, L. Núñez, C. Villalobos, Non-steroidal anti-inflammatory drugs (NSAIDs) and neuroprotection in the elderly: a view from the mitochondria, Neural Regen. Res. 10 (2015) 1371–1372.
[6] H. Zhang, L. Wu, E. Pchitskaya, O. Zakharova, T. Saito, T. Saido, I. Bezprozvanny, Neuronal store-operated calcium entry and mushroom spine loss in amyloid precursor

protein knock-in mouse model of Alzheimer's disease, J. Neurosci. 35 (2015) 13275–13286.
[7] A.B. Parekh, J.W. Putney, Store-operated calcium channels, Physiol. Rev. 85 (2005) 757–810.
[8] J. Liou, M.L. Kim, W.D. Heo, J.T. Jones, J.W. Myers, J.E. Ferrell, T. Meyer, STIM is a Ca^{2+} sensor essential for Ca^{2+}-store-depletion-triggered Ca^{2+} influx, Curr. Biol. 15 (2005) 1235–1241.
[9] S. Feske, G. Gwack, M. Prakriya, S. Srikanth, S.H. Puppel, B. Tanasa, P.G. Hogan, R.S. Lewis, M. Daly, A. Rao, A mutation in Orai1 causes immune deficiency by abrogating CRAC channel function, Nature 441 (2006) 179–185.
[10] P.G. Hogan, R.S. Lewis, A. Rao, Molecular basis of calcium signaling in lymphocytes: STIM and ORAI, Annu. Rev. Immunol. 28 (2010) 491–533.
[11] C. Villalobos, J. García-Sancho, Capacitative Ca^{2+} entry contributes to the calcium influx induced by thyrotropin-releasing hormone (TRH) in GH_3 pituitary cells, Pflugers Arch. 430 (1995) 923–935.
[12] A. Berna-Erro, A. Braun, R. Kraft, C. Kleinschnitz, M.K. Schuhmann, D. Stegner, T. Wultsch, J. Eilers, S.G. Meuth, G. Stoll, B. Nieswandt, STIM2 regulates capacitive Ca^{2+} entry in neurons and plays a key role in hypoxic neuronal cell death, Sci. Signal. 2 (93) (2009) ra67.
[13] J. Gruszczynska-Biegala, P. Pomorski, M.B. Wisniewska, J. Kuznicki, Differential roles for STIM1 and STIM2 in store-operated calcium entry in rat neurons, PLoS One 6 (4) (2011), e19285.
[14] S. Sanz-Blasco, R.A. Valero, I. Rodríguez-Crespo, C. Villalobos, L. Núñez, Mitochondrial Ca^{2+} overload underlies Aβ oligomers neurotoxicity providing an unexpected mechanism of neuroprotection by NSAIDs, PLoS One 3 (7) (2008), e2718.
[15] L.E. Jensen, G. Bultynck, T. Luyten, H. Amijee, M.D. Bootman, H.L. Roderick, Alzheimer's disease-associated peptide $Aβ_{42}$ mobilizes ER Ca^{2+} via $InsP_3R$-dependent and -independent mechanisms, Front. Mol. Neurosci. 6 (2013) 36.
[16] I.L. Ferreira, E. Ferreiro, J. Schmidt, J.M. Cardoso, C.M. Pereira, A.L. Carvalho, C.R. Oliveira, A.C. Rego, Aβ and NMDAR activation cause mitochondrial dysfunction involving ER calcium release, Neurobiol. Aging 36 (2015) 680–692.
[17] C. Villalobos, L. Núñez, P. Chamero, M.T. Alonso, J. García-Sancho, Mitochondrial $[Ca^{2+}]$ oscillations driven by local high-$[Ca^{2+}]$ domains generated by spontaneous electric activity, J. Biol. Chem. 276 (2001) 40293–40297.
[18] C. Villalobos, L. Núñez, M. Montero, A.G. García, M.T. Alonso, P. Chamero, J. Alvarez, J. García-Sancho, Redistribution of Ca^{2+} among cytosol and organella during stimulation of bovine chromaffin cells, FASEB J. 16 (2002) 343–353.
[19] L. Núñez, L. Senovilla, S.I. Sanz-Blasco, P. Chamero, M.T. Alonso, C. Villalobos, J. García-Sancho, Bioluminescence imaging of mitochondrial calcium in sympathetic neurons from adult rat dorsal root ganglion, J. Physiol. Lond. 580 (2007) 385–395.
[20] L. Núñez, C. Villalobos, J. García-Sancho, Coupling or not coupling of mitochondria to Ca^{2+} sources in neurones. Soma and neurites differ, Physiol. News 70 (2008) 23–24.
[21] R. Rizzuto, P. Pinton, W. Carrington, F.S. Fay, K.E. Fogarty, L.M. Lifshitz, R.A. Tuft, T. Pozzan, Close contacts with the endoplasmic reticulum as determinants of mitochondrial Ca^{2+} responses, Science 280 (1998) 1763–1766.
[22] C. Giorgi, D. De Stefani, A. Bononi, R. Rizzuto, P. Pinton, Structural and functional link between the mitochondrial network and the endoplasmic reticulum, Int. J. Biochem. Cell Biol. 41 (2009) 1817–1827.
[23] C. Giorgi, S. Missiroli, S. Patergnani, J. Duszynski, M.R. Wieckowski, P. Pinton, Mitochondria-associated membranes: composition, molecular mechanisms, and physiopathological implications, Antioxid. Redox Signal. 22 (2015) 995–1019.
[24] C. Cárdenas, R.A. Miller, I. Smith, T. Bui, J. Molgó, M. Müller, H. Vais, K.H. Cheung, J. Yang, I. Parker, C.B. Thompson, M.J. Birnbaum, K.R. Hallows, J.K. Foskett, Essential regulation of cell bioenergetics by constitutive $InsP_3$ receptor Ca^{2+} transfer to mitochondria, Cell 142 (2010) 270–283.
[25] W. Dong, S. Cheng, F. Huang, W. Fan, Y. Chen, H. Shi, H. He, Mitochondrial dysfunction in long-term neuronal cultures mimics changes with aging, Med. Sci. Monit. 17 (2011) BR91–BR96.
[26] G.J. Brewer, J.R. Torricelli, E.K. Evege, P.J. Price, Optimized survival of hippocampal neurons in B27-supplemented neurobasal, a new serum-free medium combination, J. Neurosci. Res. 35 (1993) 567–576.
[27] I. Pérez-Otaño, R. Luján, S.J. Tavalin, M. Plomann, J. Modregger, X.B. Liu, E.G. Jones, S.F. Heinemann, D.C. Lo, M.D. Ehlers, Endocytosis and synaptic removal of NR3A-containing NMDA receptors by PACSIN1/syndapin1, Nat. Neurosci. 9 (2006) (2006) 611–621.
[28] M. Calvo-Rodríguez, C. Villalobos, L. Núñez, Fluorescence and bioluminescence imaging of subcellular Ca^{2+} in aged hippocampal neurons, J. Vis. Exp. 106 (2015), e53330.
[29] G. Grynkiewicz, M. Poenie, R.Y. Tsien, A new generation of Ca^{2+} indicators with greatly improved fluorescence properties, J. Biol. Chem. 260 (1985) 3440–3450.
[30] M. Montero, M.T. Alonso, E. Carnicero, I. Cuchillo-Ibañez, A. Albillos, A.G. García, J. García-Sancho, J. Alvarez, Chromaffin-cell stimulation triggers fast millimolar mitochondrial Ca^{2+} transients that modulate secretion, Nat. Cell Biol. 2 (2000) 57–61.
[31] R.A. Valero, L. Senovilla, L. Núñez, C. Villalobos, The role of mitochondrial potential in control of calcium signals involved in cell proliferation, Cell Calcium 44 (2008) 259–269.
[32] J.M. Baughman, F. Perocchi, H.S. Girgis, M. Plovanich, C.A. Belcher-Timme, Y. Sancak, X.R. Bao, L. Strittmatter, O. Goldberger, R.L. Bogorad, V. Koteliansky, V.K. Mootha, Integrative genomics identifies MCU as an essential component of the mitochondrial calcium uniporter, Nature 476 (2011) 341–345.
[33] D. De Stefani, A. Raffaello, E. Teardo, I. Szabò, R. Rizzuto, A forty-kilodalton protein of the inner membrane is the mitochondrial calcium uniporter, Nature 476 (2011) 336–340.
[34] S. Sun, H. Zhang, J. Liu, E. Popugaeva, N.J. Xu, S. Feske, C.L. White 3rd., I. Bezprozvanny, Reduced synaptic STIM2 expression and impaired store-operated calcium entry cause destabilization of mature spines in mutant presenilin mice, Neuron 82 (2014) 79–93.
[35] J. Bourne, K.M. Harris, Do thin spines learn to be mushroom spines that remember? Curr. Opin. Neurobiol. 17 (2007) (2007) 381–386.
[36] M. Hoth, C.M. Fanger, R.S. Lewis, Mitochondrial regulation of store-operated calcium signaling in T lymphocytes, J. Cell Biol. 137 (1997) 633–648.
[37] J.A. Gilabert, A.B. Parekh, Respiring mitochondria determine the pattern of activation and inactivation of the store-operated Ca^{2+} current I_{CRAC}, EMBO J. 19 (2000) 6401–6407.
[38] L. Núñez, R.A. Valero, L. Senovilla, S. Sanz-Blasco, J. García-Sancho, C. Villalobos, Cell proliferation depends on mitochondrial Ca^{2+} uptake: inhibition by salicylate, J. Physiol. Lond. 571 (2006) 57–73.
[39] D. Riascos, D. de Leon, A. Baker-Nigh, A. Nicholas, R. Yukhananov, J. Bu, C.K. Wu, C. Geula, Age-related loss of calcium buffering and selective neuronal vulnerability in Alzheimer's disease, Acta Neuropathol. 122 (2011) 565–576.
[40] S.S. Ahmadian, A. Rezvanian, M. Peterson, S. Weintraub, E.H. Bigio, M.M. Mesulam, C. Geula, Loss of calbindin-D 28K is associated with the full range of tangle pathology within basal forebrain cholinergic neurons in Alzheimer's disease, Neurobiol. Aging 36 (2015) 3163–3170.
[41] E. Zampese, C. Fasolato, M.J. Kipanyula, M. Bortolozzi, T. Pozzan, P. Pizzo, Presenilin 2 modulates endoplasmic reticulum (ER)-mitochondria interactions and Ca^{2+} cross-talk, Proc. Natl. Acad. Sci. U. S. A. 108 (2011) 2777–2782.
[42] L. Hedskog, C.M. Pinho, R. Filadi, A. Rönnbäck, L. Hertwig, B. Wiehager, P. Larssen, S. Gellhaar, A. Sandebring, M. Westerlund, C. Graff, B. Winblad, D. Galter, H. Behbahani, P. Pizzo, E. Glaser, M. Ankarcrona, Modulation of the endoplasmic reticulum-mitochondria interface in Alzheimer's disease and related models, Proc. Natl. Acad. Sci. U. S. A. 110 (2013) 7916–7921.